

Trapping of Three-Center Ir-Sn-X Intermediates in the Reaction of Ir^I[C₆H₄(CH₂NMe₂)₂](COD) with Organotin(IV) Halides. X-ray Structure of [2-(Me₂NCH₂)C₆H₄](COD)Ir(Br)SnMe₂Br

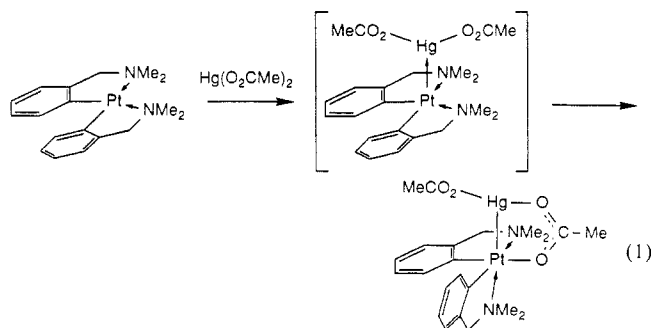
Adolphus A. H. van der Zeijden,[†] Gerard van Koten,^{*,†} Jacqueline M. A. Wouters,[†] Willem F. A. Wijsmuller,[†] David M. Grove,[†] Wilberth J. J. Smeets,[‡] and Anthony L. Spek[‡]

Contribution from the Anorganisch Chemisch Laboratorium, University of Amsterdam, Nieuwe Achtergracht 166, 1018 WV Amsterdam, The Netherlands, and Vakgroep Algemene Chemie, Afdeling Kristal- en Structuurchemie, University of Utrecht, Padualaan 8, 3584 CH Utrecht, The Netherlands. Received November 5, 1987

Abstract: The reaction of Ir^I[C₆H₄(CH₂NMe₂)₂](COD) with various organotin(IV) halides SnRR'₂X₂ yields dinuclear adducts [2-(Me₂NCH₂)C₆H₄](COD)Ir(X)SnRR'₂X (X = Cl, R = R' = Me, Ph; X = R = Cl, R' = Me; X = Br, R = R' = Me, Br; X = Br, R = Me, R' = Ph). No reaction was observed with SnMe₃Cl. The X-ray structure of [2-(Me₂NCH₂)C₆H₄](COD)Ir(Br)SnMe₂Br was determined. Crystals are triclinic, space group *P* $\bar{1}$, with unit-cell dimensions *a* = 10.122 (2) Å, *b* = 14.136 (2) Å, *c* = 17.310 (2) Å, α = 66.83 (1)°, β = 69.35 (1)°, γ = 73.64 (2)°. The crystal structure was solved with direct methods (Ir, Sn, Br) and subsequent difference Fourier techniques. Anisotropic blocked full-matrix least-squares refinement with 6605 observed reflections and 458 parameters converged at *R*_F = 0.0337. The molecule contains an Ir-Sn-Br triangle, which appears to be the result of an Sn-Br bond that is side-on coordinated to Ir. As such it can be envisaged as a unique "trapped" three-center intermediate in the concerted oxidative addition of a metal-halide bond to a square-planar metal d⁸ complex.

Oxidative addition is a collective term for various means of electron transfer from a metal center to a substrate. Several mechanisms for this process, which is accompanied by quite dramatic changes in the electronic and geometric environment of the metal, have been proposed.¹ In a particular case, the type of mechanism that occurs has been found to be very sensitive to many factors including the nature of the metal complex, the substrate, and the solvent.¹ With d⁸ metal complexes the addition mechanisms of dihydrogen, silanes, hydrogen halides, and alkyl halides have been much studied, but those of halogens and metal halides less so. It has been shown that, in general, concerted cis addition takes place for dihydrogen and silanes, while for the other cases several mechanisms, all involving electrophilic attack of the substrate on the nucleophilic metal center, have been proposed.¹

Both cis and trans oxidative additions of metal (pseudo)halides (especially d¹⁰ Hg^{II}, Tl^{III}, and Sn^{IV} salts) to d⁸ metal complexes have long been known.^{2,3} For example, the complex [2-(Me₂NCH₂)C₆H₄]₂Pt(μ-O₂CMe)Hg(O₂CMe) (eq 1), isolated by



Van der Ploeg et al., can be considered as a "trapped" intermediate in the concerted cis addition of a mercury-acetate bond to *cis*-Pt^{II}[C₆H₄(CH₂NMe₂)₂]₂.⁴ The first step in this reaction was thought to be the formation of an intermediate adduct with a

donative Pt to Hg bond (eq 1). In the case of *trans*-Pt^{II}[C₆H₄(CH₂NMe₂)₂]₂, an adduct of this type was indeed observed, but further reaction led to elimination of Hg⁰ and formation of Pt^{IV}(O₂CMe)₂[C₆H₄(CH₂NMe₂)₂]₂.⁴

The fact that such platinum-mercury species can be detected, and sometimes even be isolated, can be attributed to the presence of the chelating ortho-CH₂NMe₂-substituted aryl ligands which provide some protection against low-energy decomposition pathways and further reactions. The use of this type of ligand has been recently extended to rhodium and iridium, and d⁸ Rh^I and Ir^I derivatives, especially, were found to be very reactive toward a variety of electrophiles. Oxidative addition, not accompanied by M-C bond cleavage, occurs with Rh^I[C₆H₃(CH₂NMe₂)₂-2,6](COD) (COD = 1,5-cyclooctadiene) and MeI, yielding Rh^{III}(Me)I[C₆H₃(CH₂NMe₂)₂-2,6],⁵ and with Ir^I[C₆H₄(CH₂NMe₂)₂](COD) and H₂, yielding Ir^{III}H₂[C₆H₄(CH₂NMe₂)₂](COD) (stable below 0 °C).⁶ The complex Rh^I[C₆H₃(CH₂NMe₂)₂-2,6](COD) also reacts with a variety of metal salts, resulting in either M-C bond cleavage (transmetalation) with Hg^{II} and Sn^{IV} halides or oxidation of the metal center without M-C bond cleavage with Ag^I salts.⁷ The mechanisms operating for the former transmetalation reactions were thought not to be based on the rhodium center but rather to proceed through electrophilic attack of the metal salt on the Rh-C(aryl) bond or on the C(aryl) atom itself.⁷ In this paper we report the reaction of related Ir^I[C₆H₄(CH₂NMe₂)₂](COD) with organotin(IV) halides that affords unique iridium-tin adducts

* To whom correspondence should be addressed at the Laboratory of Organic Chemistry, University of Utrecht, Dept. of Metal Mediated Synthesis, Padualaan 8, 3584 CH Utrecht, The Netherlands.

[†]University of Amsterdam.

[‡]University of Utrecht.

(1) (a) Chock, P. B.; Halpern, J. *J. Am. Chem. Soc.* **1966**, *88*, 3511. (b) Collman, J. P.; Roper, W. R. *Adv. Organomet. Chem.* **1968**, *7*, 53. (c) Stille, J. K.; Lau, K. S. Y. *Acc. Chem. Res.* **1977**, *10*, 434. (d) Atwood, J. D. *Inorganic and Organometallic Reaction Mechanisms*; Brooks/Cole: Monterey, 1985; pp 162-192.

(2) Nyholm, R. S.; Vrieze, K. *J. Chem. Soc.* **1965**, 5337.

(3) Taylor, R. C.; Young, J. F.; Wilkinson, G. *Inorg. Chem.* **1966**, *5*, 20.

(4) van der Ploeg, A. F. M. J.; van Koten, G.; Vrieze, K.; Spek, A. L. *Inorg. Chem.* **1982**, *21*, 2014.

(5) van der Zeijden, A. A. H.; van Koten, G.; Ernsting, J. M.; Krijnen, B.; Stam, C. H. *J. Chem. Soc., Dalton Trans.*, accepted for publication.

(6) van der Zeijden, A. A. H.; van Koten, G.; Luijk, R.; Grove, D. M. *Organometallics*, in press.

(7) van der Zeijden, A. A. H.; van Koten, G.; Nordemann, R. A.; Kojić-Prodrić, B.; Spek, A. L. *Organometallics*, in press.

which can be regarded as "trapped" intermediates in the concerted cis oxidative addition of a tin-halide bond to an iridium(I) center.

Experimental Section

General Methods. All manipulations were performed at room temperature under an atmosphere of nitrogen with use of Schlenk techniques. $\text{Ir}[\text{C}_6\text{H}_3(\text{CH}_2\text{NMe}_2)\text{-2-R-6}](\text{COD})$ (R = H, Me, CH_2NMe_2) were prepared according to ref 8. Solvents were carefully dried and distilled prior to use. ^1H NMR spectra were recorded on a Bruker WM250 spectrometer. Elemental analyses were carried out by the Analytical Department of the Institute for Applied Chemistry, TNO, Zeist, The Netherlands. Molecular weights were determined in CH_2Cl_2 by using a HP 320B vapor pressure osmometer (estimated error: $\pm 10\%$, $c = 0.01$ mol/L).

Synthesis of $[2\text{-}(\text{Me}_2\text{NCH}_2)\text{C}_6\text{H}_4](\text{COD})\text{Ir}(\text{X})\text{SnRR}'\text{X}$ (1-6). To a stirred solution of $\text{Ir}[\text{C}_6\text{H}_4(\text{CH}_2\text{NMe}_2)\text{-2}](\text{COD})$ (ca. 50 mg) in benzene or toluene (5 mL) was added an equimolar quantity of $\text{SnRR}'\text{X}_2$. Within a few seconds the red solution became pale yellow and within 5-60 min a yellow solid was deposited (with SnBr_4 a red solid precipitated instantaneously). This solid was filtered off, washed with pentane (5 mL), and dried in vacuo: yield 60-90%. The compounds are moderately air-stable. $\text{Ir}[\text{C}_6\text{H}_4(\text{CH}_2\text{NMe}_2)\text{-2}](\text{COD})$ did not react with SnMe_3Cl under these conditions.

$[2\text{-}(\text{Me}_2\text{NCH}_2)\text{C}_6\text{H}_4](\text{COD})\text{Ir}(\text{Cl})\text{SnMe}_2\text{Cl}$ (1): mol wt calcd 654, found 607.

$[2\text{-}(\text{Me}_2\text{NCH}_2)\text{C}_6\text{H}_4](\text{COD})\text{Ir}(\text{Br})\text{SnMe}_2\text{Br}$ (2): mol wt calcd 743, found 701. Anal. Calcd for $\text{C}_{19}\text{H}_{30}\text{Br}_2\text{IrNSn}$: C, 30.71; H, 4.07; Br, 21.50; N, 1.89. Found: C, 30.56; H, 4.23; Br, 21.40; N, 2.05. Crystals of the complex, suitable for a single-crystal X-ray diffraction study, were formed from a freshly prepared 1:1 mixture of $\text{Ir}[\text{C}_6\text{H}_4(\text{CH}_2\text{NMe}_2)\text{-2}](\text{COD})$ and SnMe_2Br_2 in benzene upon standing for a few hours.

$[2\text{-}(\text{Me}_2\text{NCH}_2)\text{C}_6\text{H}_4](\text{COD})\text{Ir}(\text{Cl})\text{SnPh}_2\text{Cl}$ (3): mol wt calcd 778, found 787. Anal. Calcd for $\text{C}_{29}\text{H}_{34}\text{Cl}_2\text{IrNSn}$: C, 44.75; H, 4.40; Cl, 9.11; N, 1.80. Found: C, 44.65; H, 4.59; Cl, 8.77; N, 1.74.

$[2\text{-}(\text{Me}_2\text{NCH}_2)\text{C}_6\text{H}_4](\text{COD})\text{Ir}(\text{Br})\text{SnMePhBr}$ (4): Anal. Calcd for $\text{C}_{24}\text{H}_{32}\text{Br}_2\text{IrNSn}$: C, 35.80; H, 4.01; Br, 19.85; N, 1.74. Found: C, 36.94; H, 4.34; Br, 20.15; N, 1.58.

$[2\text{-}(\text{Me}_2\text{NCH}_2)\text{C}_6\text{H}_4](\text{COD})\text{Ir}(\text{Cl})\text{SnMeCl}_2$ (5): Anal. Calcd for $\text{C}_{18}\text{H}_{27}\text{Cl}_3\text{IrNSn}$: C, 32.04; H, 4.03; Cl, 15.76; N, 2.08. Found: C, 32.57; H, 4.38; Cl, 15.28; N, 1.98.

$[2\text{-}(\text{Me}_2\text{NCH}_2)\text{C}_6\text{H}_4](\text{COD})\text{Ir}(\text{Br})\text{SnBr}_3$ (6): Anal. Calcd for $\text{C}_{17}\text{H}_{24}\text{Br}_4\text{IrNSn}$: C, 23.39; H, 2.77; Br, 36.61; N, 1.60. Found: C, 23.39; H, 3.21; Br, 36.06; N, 1.55.

Decomposition of $[2\text{-}(\text{Me}_2\text{NCH}_2)\text{C}_6\text{H}_4](\text{COD})\text{Ir}(\text{Br})\text{SnMe}_2\text{Br}$ (2). A freshly prepared solution of $\text{Ir}[\text{C}_6\text{H}_4(\text{CH}_2\text{NMe}_2)\text{-2}](\text{COD})$ (ca. 100 mg) and an equimolar amount of SnMe_2Br_2 in benzene (3 mL) was stirred for 3 days. The off-white precipitate which was formed was filtered off; it probably contained polymeric organotin compounds. The orange filtrate was found to contain a 1:2 mixture of $[\text{IrBr}(\text{COD})]_2$ and $\text{C}_6\text{H}_5\text{CH}_2\text{NMe}_2$ (^1H NMR); the resonances of the 1:1 iridium-tin adduct 2 had disappeared. To this orange filtrate was added 1 N hydrochloric acid (5 mL), and after stirring for a few minutes, the two layers were separated. The benzene layer afforded, after evaporation of the solvent, quantitatively $[\text{IrBr}(\text{COD})]_2$ (identified by ^1H NMR and FD mass spectroscopy). The water layer afforded the white ammonium salt $[\text{C}_6\text{H}_5\text{CH}_2\text{N}(\text{H})\text{Me}_2]\text{Cl}$ in quantitative yield.

The behavior of the other iridium-tin complexes 1 and 3-6 in either C_6D_6 or CD_2Cl_2 was monitored by ^1H NMR. The tin-methyl complexes 1, 4, and 5 showed at about the same rate a similar product formation as found for 2. No decomposition was observed either for 3 or for 6. The latter complex was also recovered unchanged after stirring for 3 weeks as a suspension in pyridine.

Reaction of $\text{Ir}[\text{C}_6\text{H}_3(\text{CH}_2\text{NMe}_2)\text{-2-R-6}](\text{COD})$ (R = Me, CH_2NMe_2) with SnMe_2Br_2 . This reaction was conducted as described above for the decomposition of $[2\text{-}(\text{Me}_2\text{NCH}_2)\text{C}_6\text{H}_4](\text{COD})\text{Ir}(\text{Br})\text{SnMe}_2\text{Br}$. An instant reaction took place, affording an insoluble white solid (probably containing organotin polymers). The benzene filtrate yielded $[\text{IrBr}(\text{COD})]_2$ quantitatively after workup. When R = Me, the acidic water layer afforded 100% $[1\text{-}(\text{Me}_2(\text{H})\text{NCH}_2)\text{-3-Me-C}_6\text{H}_4]\text{Cl}$. When R = CH_2NMe_2 a mixture of $[1\text{-}(\text{Me}_2(\text{H})\text{NCH}_2)_2\text{C}_6\text{H}_4]\text{Cl}_2$ (65%) and the tin salt $[\text{SnMe}_2[\text{C}_6\text{H}_3(\text{CH}_2\text{NMe}_2)_2\text{-2,6}]]\text{Cl}$ (35%) was obtained (both identified by ^1H NMR,⁹ product distribution by integration).

Structure Determination and Refinement of $[2\text{-}(\text{Me}_2\text{NCH}_2)\text{C}_6\text{H}_4](\text{COD})\text{Ir}(\text{Br})\text{SnMe}_2\text{Br}$ (2). A yellow plate shaped crystal was mounted on a glass fiber and transferred to an ENRAF-Nonius CAD-4F diffractometer for data collection. Crystal data and details of the structure

Table I. Crystal Data and Details of the Structure Analysis of $[2\text{-}(\text{Me}_2\text{NCH}_2)\text{C}_6\text{H}_4](\text{COD})\text{Ir}(\text{Br})\text{SnMe}_2\text{Br}$

a. Crystal Data (294 K)	
formula	$\text{C}_{19}\text{H}_{30}\text{NBr}_2\text{IrSn}$
mol wt	743.17
cryst system	triclinic
space group	$P\bar{1}$ (no. 2)
a, b, c (Å)	10.122 (2), 14.136 (2), 17.310 (2)
α, β, γ (deg)	66.83 (1), 69.35 (1), 73.64 (2)
V (Å ³)	2101.1(8)
Z	4
D_{calcd} (g cm ⁻³)	2.349
$F(000)$	1392
μ (Mo K α) (cm ⁻¹)	112.7
cryst size (mm)	$0.43 \times 0.28 \times 0.13$
b. Data Collection (294 K)	
$\Theta_{\text{min}}, \Theta_{\text{max}}$ (deg)	1.9, 27.5
radiation	Zr-filtered Mo K α , 0.71073 Å
$\omega/2\theta$ scan (deg)	$0.70 + 0.35 \tan \Theta$
horzntl and vert aperture (mm)	4.0, 4.0
distance cryst to detector (mm)	173
ref reflns	113, -111, 111
total data	8742
unique data	8291
obsd data ($I > 2\sigma(I)$)	6605
c. Refinement	
no. of refined params	458
weighting scheme	$w = 1/\sigma^2(F)$
final R, R_w, S	0.0337, 0.0364, 1.35
$(\Delta/\sigma)_{\text{av}}$ in final cycle	0.009

determination are given in Table I. Unit cell parameters were determined from a least-squares treatment of the setting angles of 22 reflections in the range $11.4 < \theta < 14.2^\circ$. The triclinic unit cell was checked for the presence of higher lattice symmetry.^{10b} Data were collected for one hemisphere ($-13 \leq h \leq 0, -13 \leq k \leq 13, -18 \leq l \leq 18$) and corrected for Lp, absorption (Gaussian integration: grid $10 \times 10 \times 10$; maximum and minimum correction: 14.256 and 3.938), and for a linear decay of 3.3% during 187 h of X-ray exposure. Standard deviations based on counting statistics were increased according to an analysis of the excess variance of three reference reflections: $\sigma^2(I) = \sigma_{\text{cs}}^2(I) + (0.054I)^2$.^{10a} Space group $P\bar{1}$ was discriminated from $P1$ during the structure determination process. The equivalent reflections ($0k1$ and $0\bar{k}1$) were merged with a consistency index (on I) of 5.54%. The Ir, Sn, and Br atoms were found with direct methods (SHELXS86);^{10b} other non-H atoms were located from subsequent difference Fourier maps. Refinement was carried out by blocked full-matrix least-squares techniques (on F) with anisotropic thermal parameters for all non-H atoms. Hydrogen atoms were introduced on calculated positions [$d(\text{C-H}) = 0.98$ Å] and included in the refinement riding on their carrier atom with one common isotropic thermal parameter. Weights were introduced in the final refinement cycles; convergence was reached at $R_F = 0.0337$. Final positional parameters are listed in Table II. A final difference Fourier synthesis reveals residual density (interpreted as absorption artefact) of $2.92 \text{ e}\text{\AA}^{-3}$ at 1.05 Å from Ir(1) (molecule 2); all other features are between 1.34 and $-1.46 \text{ e}\text{\AA}^{-3}$. Neutral atom scattering factors were taken from ref 10c and corrected for anomalous dispersion.^{10d} Data collection was done with a modified CAD-4F software package.^{10e} All calculations were performed with SHELX76^{10f} and the EUCLID package^{10g} (geometrical calculations and illustrations) on the CDC Cyber-855 of the University of Utrecht.

Results

Synthesis of $[2\text{-}(\text{Me}_2\text{NCH}_2)\text{C}_6\text{H}_4](\text{COD})\text{Ir}(\text{X})\text{SnRR}'\text{X}$ (1-6). The reaction of the square-planar iridium(I) complex $\text{Ir}[\text{C}_6\text{H}_4\text{-}$

(10) (a) McCandlish, L. E.; Stout, G. H.; Andrews, L. C. *Acta Crystallogr., Sect. A: Cryst. Phys., Diffr., Theor. Gen. Crystallogr.* **1975**, *A31*, 245. (b) Sheldrick, G. M. SHELXS86, program for crystal structure determination, University of Goettingen, FRG, 1986. (c) Cromer, D. T.; Mann, J. B. *Acta Crystallogr., Sect. A: Cryst. Phys., Diffr., Theor. Gen. Crystallogr.* **1968**, *A24*, 321. (d) Cromer, D. T.; Liberman, D. *J. Chem. Phys.* **1970**, *53*, 1891. (e) de Boer, J. L.; Duisenberg, A. J. M. *Acta Crystallogr., Sect. A: Found. Crystallogr.* **1984**, *A40*, C410. (f) Sheldrick, G. M. SHELX76, crystal structure analysis package, University of Cambridge, 1976. (g) Spek, A. L. The EUCLID package In *Computational Crystallography*; Sayre, D., Ed.; Clarendon Press: Oxford, 1982; p 528. (h) Le Page, Y. *J. Appl. Cryst.* **1982**, *15*, 255.

(8) van der Zeijden, A. A. H.; van Koten, G.; Luijk, R.; Nordemann, R. A.; Spek, A. L. *Organometallics*, in press.

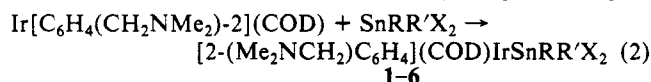
(9) van Koten, G.; Jastrzebski, J. T. B. H.; Noltes, J. G.; Spek, A. L.; Schoone, J. C. *J. Organomet. Chem.* **1978**, *148*, 233.

Table II. Positional and Equivalent Isotropic Thermal Parameters of $[2-(\text{Me}_2\text{NCH}_2)_2\text{C}_6\text{H}_4](\text{COD})\text{Ir}(\text{Br})\text{SnMe}_2\text{Br}$

atom	x	y	z	U (eq), ^a Å ²
Molecule 1				
Ir(1)	0.65914 (3)	0.22601 (2)	0.51023 (2)	0.0246 (1)
Sn(1)	0.39949 (5)	0.22127 (4)	0.61738 (3)	0.0304 (2)
Br(1)	0.58781 (8)	0.36399 (6)	0.58707 (5)	0.0389 (3)
Br(2)	0.27533 (9)	0.06958 (7)	0.64128 (6)	0.0517 (3)
N(1)	0.8944 (6)	0.2318 (5)	0.5019 (4)	0.035 (2)
C(1)	0.7072 (7)	0.0970 (5)	0.6132 (4)	0.028 (2)
C(2)	0.8191 (7)	0.0992 (6)	0.6414 (5)	0.034 (2)
C(3)	0.8655 (8)	0.0154 (6)	0.7076 (5)	0.044 (3)
C(4)	0.8062 (9)	-0.0720 (6)	0.7455 (5)	0.050 (3)
C(5)	0.6955 (8)	-0.0801 (6)	0.7188 (5)	0.039 (2)
C(6)	0.6486 (7)	0.0047 (5)	0.6537 (4)	0.032 (2)
C(7)	0.8905 (8)	0.1918 (6)	0.5959 (5)	0.040 (3)
C(8)	1.0060 (8)	0.1596 (7)	0.4622 (6)	0.050 (3)
C(9)	0.9417 (9)	0.3346 (6)	0.4623 (6)	0.048 (3)
C(10)	0.3784 (9)	0.1829 (7)	0.7531 (5)	0.049 (3)
C(11)	0.2316 (8)	0.3472 (6)	0.5774 (5)	0.046 (3)
C(12)	0.792 (1)	0.3155 (6)	0.3106 (5)	0.052 (3)
C(13)	0.7939 (9)	0.1988 (6)	0.3295 (5)	0.046 (3)
C(14)	0.7369 (8)	0.1362 (6)	0.4242 (5)	0.039 (3)
C(15)	0.5899 (8)	0.1308 (5)	0.4639 (5)	0.035 (3)
C(16)	0.4769 (9)	0.1878 (6)	0.4149 (5)	0.046 (3)
C(17)	0.480 (1)	0.3042 (6)	0.3691 (5)	0.050 (3)
C(18)	0.5473 (8)	0.3507 (6)	0.4095 (5)	0.040 (2)
C(19)	0.6888 (9)	0.3572 (6)	0.3813 (4)	0.041 (3)
Molecule 2				
Ir(1)	0.29323 (3)	0.71655 (2)	0.08009 (2)	0.0282 (1)
Sn(1)	0.13984 (5)	0.57938 (4)	0.20741 (3)	0.0313 (2)
Br(1)	0.07447 (9)	0.80492 (6)	0.17641 (5)	0.0441 (3)
Br(2)	0.2187 (1)	0.38544 (6)	0.20837 (6)	0.0490 (3)
N(1)	0.2709 (7)	0.8791 (5)	-0.0288 (4)	0.046 (3)
C(1)	0.1817 (8)	0.6962 (6)	0.0095 (4)	0.033 (2)
C(2)	0.1119 (8)	0.7899 (6)	-0.0400 (5)	0.040 (3)
C(3)	0.036 (1)	0.7885 (7)	-0.0942 (6)	0.058 (3)
C(4)	0.0267 (9)	0.6955 (8)	-0.0981 (5)	0.057 (4)
C(5)	0.0975 (8)	0.6039 (7)	-0.0526 (5)	0.047 (3)
C(6)	0.1741 (8)	0.6048 (6)	-0.0005 (4)	0.035 (3)
C(7)	0.127 (1)	0.8895 (6)	-0.0377 (6)	0.052 (3)
C(8)	0.375 (1)	0.8814 (7)	-0.1161 (5)	0.062 (3)
C(9)	0.275 (1)	0.9731 (7)	-0.0121 (6)	0.062 (4)
C(10)	-0.0712 (8)	0.5886 (7)	0.2013 (6)	0.049 (3)
C(11)	0.1549 (8)	0.5453 (6)	0.3369 (4)	0.037 (2)
C(12)	0.579 (1)	0.7884 (8)	0.0404 (6)	0.063 (4)
C(13)	0.6194 (9)	0.7070 (7)	-0.0064 (5)	0.052 (3)
C(14)	0.4936 (8)	0.6608 (6)	0.0019 (5)	0.040 (3)
C(15)	0.4455 (7)	0.5748 (6)	0.0732 (5)	0.035 (2)
C(16)	0.5105 (8)	0.5213 (6)	0.1488 (5)	0.044 (3)
C(17)	0.5233 (8)	0.5933 (7)	0.1905 (6)	0.051 (3)
C(18)	0.4145 (8)	0.6916 (7)	0.1801 (5)	0.043 (3)
C(19)	0.4404 (8)	0.7837 (7)	0.1092 (5)	0.044 (3)

$$^a U(\text{eq}) = \frac{1}{3} \sum_{ij} U_{ij} a_i^* a_j^* a_i a_j$$

$(\text{CH}_2\text{NMe}_2)_2(\text{COD})^8$ with an equimolar amount of $\text{SnRR}'\text{X}_2$ in either benzene, toluene, or CH_2Cl_2 results within 5–60 min in the formation of a yellow precipitate (red for SnBr_4). These solid products were identified, by a combination of elemental analyses, osmometric measurements in CH_2Cl_2 , and ^1H NMR, as being monomeric 1:1 adducts of the two starting compounds (eq 2).



X =, R =, R' =: (1) Cl, Me, Me;

(2) Br, Me, Me; (3) Cl, Ph, Ph; (4) Br, Me, Ph;

(5) Cl, Me, Cl; (6) Br, Br, Br;

The presence of at least two halide atoms on tin appears to be a prerequisite for this adduct formation, since no reaction was observed with this iridium complex and the triorganotin compound SnMe_3Cl . It was also observed that the more halide atoms there were present, the faster adduct formation proceeded. The moderately air-stable adducts are slightly soluble in CH_2Cl_2 and benzene; as the number of tin-bonded halide atoms present in-

creases, so the solubility of the complex decreases.

^1H NMR Spectroscopic Measurements. The ^1H NMR spectral data of the iridium–tin complexes 1–6 measured in CD_2Cl_2 at room temperature are listed in Table III. The resonance patterns of the $[\text{C}_6\text{H}_4(\text{CH}_2\text{NMe}_2)_2]$ and COD ligands indicate a lack of molecular symmetry, and in this respect these adducts resemble the iridium(III) dihydride $\text{IrH}_2[\text{C}_6\text{H}_4(\text{CH}_2\text{NMe}_2)_2](\text{COD})$.⁶ From the appearance of the two benzylic protons as two well-separated AX doublets and of the two NMe_2 methyls as two singlet resonances, it is concluded that the respective C and N centers are diastereotopic. The chirality of the tertiary amine group indicates that the N-atom is coordinated to iridium. The four olefinic protons of COD appear as four separate (sometimes overlapping) resonances between 3.4 and 5.4 ppm.

In the SnMe_2X_2 adducts 1 and 2 there are two singlet resonances between 0.3 and 1.1 ppm, having $^2J(\text{Sn}-\text{H})$ couplings that are characteristic for tin-bonded methyl groups.¹¹ The fact that the prochiral SnMe_2 entity affords two separate methyl resonances indicates that the tin center is in some way bonded to the $[\text{C}_6\text{H}_4(\text{CH}_2\text{NMe}_2)_2](\text{COD})$ system, most probably to the iridium center. Consequently, in those adducts where the R and R' groups of $\text{SnRR}'\text{X}_2$ are not the same, as in 4 (SnMePhBr_2) and 5 (SnMeCl_3), one can reason on symmetry grounds that two isomers should be possible. For complex 4, these are indeed observed (designated 4a and 4b in Table III; 4a:4b = 2:1), but for 5 only one of the isomers appears to be present. These different and unequal isomer distributions in 4 and 5 point to significant steric and/or electronic differences in the surroundings of the R and R' sites in these complexes.

With respect to the parent tin compounds, the resonances of the SnMe groups in the adducts 1, 2, 4a/b, and 5 show upfield chemical shifts that consistently fall into two narrowly defined ranges (see Table III). These ranges of +0.83 (± 0.08) (Δ), and +0.27 (± 0.02) (Δ') ppm have associated $^2J(\text{Sn}-\text{H})$ couplings of ca. 63 and 49 Hz, respectively (separate ^{117}Sn and ^{119}Sn couplings were not observed at 250 MHz). These data relate clearly to the two different sites of the R and R' groups in these adducts. On this basis it can be deduced that the single SnMe group in both 4a and 5 probably resides in the same relative position. It should be noted that although the magnitudes of $^2J(\text{Sn}-\text{H})$ couplings are usually very characteristic for the coordination around tin in its normal mononuclear complexes, the proximity of another metal (Ir) may significantly influence them.¹¹

The ^1H NMR data are consistent with the presence of a direct Ir–Sn interaction in all adducts, but they are insufficient in themselves to allow an unambiguous structural deduction. Therefore an X-ray crystallographic analysis of a representative adduct, $[2-(\text{Me}_2\text{NCH}_2)_2\text{C}_6\text{H}_4](\text{COD})\text{Ir}(\text{Br})\text{SnMe}_2\text{Br}$ (2), was undertaken.

Solid-State Structure of $[2-(\text{Me}_2\text{NCH}_2)_2\text{C}_6\text{H}_4](\text{COD})\text{Ir}(\text{Br})\text{SnMe}_2\text{Br}$ (2). The crystal structure of 2 consists of four discrete molecules in a triclinic unit cell. The asymmetric unit contains two crystallographically independent molecules (numbered 1 and 2). Selected bond distances and angles are listed in Tables IV and V. The differences in the geometrical data of the two molecules are minor, and therefore only the structure of molecule 1 will be described. The structure of molecule 1 and the adopted numbering scheme is shown in Figure 1.

Iridium Coordination Sphere. The coordination sphere of iridium is supplied by two double bonds of COD, the C,N-bonded aryl ligand and by both a bromide and tin atom of a SnMe_2Br_2 unit. The midpoint of the double bond C(18)=C(19) [m(2)] and C(1) of the aryl moiety form an almost linear axial arrangement with the iridium center [C(1)–Ir(1)–m(2) = 175.4 (3)°]. Close to a meridional plane that is perpendicular to this axis and which passes through Ir(1) lies the midpoint of the other double bond C(14)=C(15) [m(1)], N(1) of the aryl ligand, and Sn(1) and

(11) (a) Harris, R. K.; Kennedy, J. D.; McFarlane, W. *NMR and the Periodic Table*; Harris, R. K., Mann, B. E., Eds.; Academic Press: London, 1978; pp 343–366. (b) Harris, D. H.; Lappert, M. F.; Poland, J. S.; McFarlane, W. *J. Chem. Soc., Dalton Trans.* 1975, 311.

Table III. ¹H NMR Data of [2-(Me₂NCH₂)C₆H₄](COD)Ir(X)SnRR'X^a

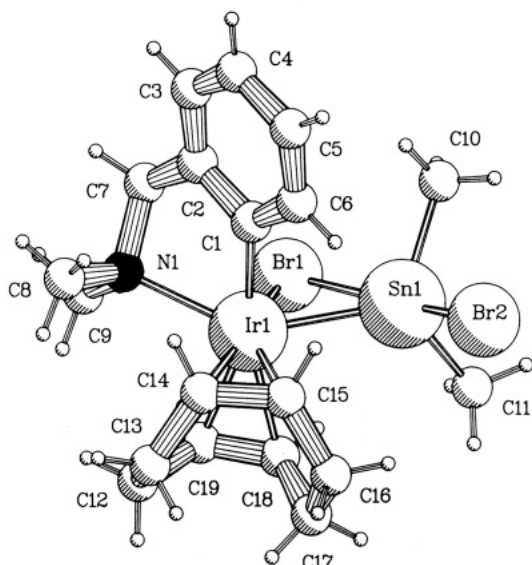
X	R	R'	[2-(Me ₂ NCH ₂)C ₆ H ₄]								COD		SnRR'				
			aryl ^b			CH ₂ ^c		NMe		=CH ^d		R ^e	R ^{e'}	Δ ^f	Δ ^{f'}		
1	Cl	Me	Me	6.94 (m)	7.12 (d)	7.70 (d)	3.18 (d)	4.91 (d)	2.58	3.05	3.49	4.27 (2 H)	4.83	0.55 (60)	1.11 (49)	0.85	0.29
2	Br	Me	Me	6.93 (m)	7.12 (d)	7.65 (d)	3.08 (d)	4.82 (d)	2.70	2.96	3.38	4.21 (2 H)	4.75	0.28 (60)	0.92 (49)	0.91	0.27
3	Cl	Ph	Ph	g	7.22 (d)	7.88 (d)	3.18 (d)	5.02 (d)	2.76	2.98	3.54	4.26	4.58	4.66	6.7-8.1 (m)		
4a	Br	Me	Ph	6.97 (m)	7.16 (d)	7.93 (d)	3.18 (d)	4.96 (d)	2.70	3.02	3.57	4.22	4.40	4.50	0.73 (63)	h	0.76
4b	Br	Ph	Me		g			g	2.74	3.07					1.24 ^g		0.25
5	Cl	Me	Cl	6.99 (m)	7.19 (d)	7.61 (d)	3.09 (d)	4.93 (d)	2.76	3.00	3.46	4.44	4.56	5.44	0.86 (67)		0.83
6	Br	Br	Br	7.03 (m)	7.22 (d)	7.60 (d)	3.18 (d)	5.16 (d)	2.74	3.08	3.73	4.19	4.82 (2 H)				

^a Measured in CD₂Cl₂ at 250 MHz; chemical shifts relative to external TMS. ^b ³J(H-H) = 7 Hz. ^c AX doublets with ²J(H-H) = 13 Hz. ^d Broad resonances. ^e ²J(Sn-H) between parentheses; ¹¹⁷Sn and ¹¹⁹Sn couplings were not resolved. ^f Δ = difference of the proton chemical shifts of SnMe, between that in the pure tin(IV) compound and the iridium-tin complex. ^g Resonances obscured. ^h 7.34 (m, para/meta), 8.01 (m, ortho).

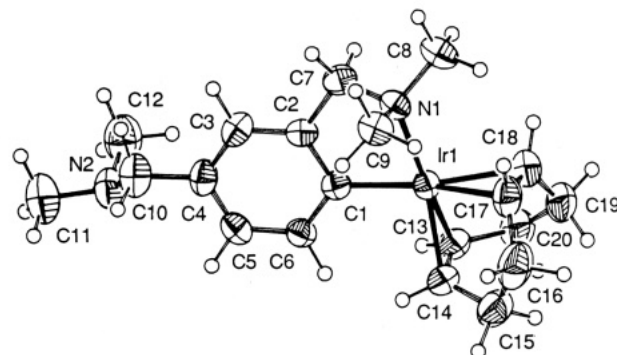
Table IV. Selected Bond Distances (Å) of [2-(Me₂NCH₂)C₆H₄](COD)Ir(Br)SnMe₂Br^a

	molecule 1	molecule 2		molecule 1	molecule 2
(a) Around Iridium					
Ir(1)-Sn(1)	2.6297 (8)	2.6358 (8)	Ir(1)-C(18)	2.297 (8)	2.324 (9)
Ir(1)-Br(1)	2.582 (1)	2.592 (1)	Ir(1)-C(19)	2.257 (7)	2.253 (9)
Ir(1)-N(1)	2.357 (7)	2.342 (7)	Ir(1)-m(1)	2.033 (8)	2.038 (9)
Ir(1)-C(1)	2.072 (7)	2.069 (8)	Ir(1)-m(2)	2.174 (8)	2.180 (9)
Ir(1)-C(14)	2.132 (8)	2.138 (8)	Ir(1)-m(3)	2.1538 (9)	2.1638 (9)
Ir(1)-C(15)	2.173 (8)	2.173 (8)			
(b) Around Tin					
Sn(1)-Br(1)	2.934 (1)	2.934 (1)	Sn(1)-C(10)	2.137 (8)	2.141 (9)
Sn(1)-Br(2)	2.608 (1)	2.626 (1)	Sn(1)-C(11)	2.166 (9)	2.152 (7)
(c) Within Aryl Ligand					
C(2)-C(7)	1.48 (1)	1.48 (1)	⟨C(sp ²)-C(sp)⟩	1.39 (2)	1.39 (2)
⟨N(1)-C⟩	1.48 (1)	1.487 (9)			
(d) Within COD Ligand					
C(14)-C(15)	1.41 (1)	1.40 (1)	⟨C(sp ²)-C(sp ³)⟩	1.52 (1)	1.51 (2)
C(18)-C(19)	1.36 (1)	1.41 (1)	⟨C(sp ³)-C(sp ³)⟩	1.54 (1)	1.53 (1)

^a m(1) is the midpoint of C(14)-C(15), m(2) is the midpoint of C(18)-C(19), and m(3) is the midpoint of Sn(1)-Br(1).

Figure 1. X-ray structure of [2-(Me₂NCH₂)C₆H₄](COD)Ir(Br)SnMe₂Br (2) (molecule 1).

Br(1) of the SnMe₂Br₂ unit. The resulting octahedral geometry is far from regular, because the four meridional interligand angles deviate significantly from 90°, i.e., m(1)-Ir(1)-Sn(1) = 101.0 (2), Sn(1)-Ir(1)-Br(1) = 68.51 (3), Br(1)-Ir(1)-N(1) = 84.1 (2), and N(1)-Ir(1)-m(1) = 110.0 (3)°. However, if the Sn(1)-Br(1) bond, with m(3) as its midpoint, is considered as one side-on coordinated ligand, the iridium center then has a fairly regular five-coordinate trigonal bipyramidal geometry. The angles in the trigonal plane, defined by Ir(1), N(1), m(1) and m(3), are then as follows: m(1)-Ir(1)-m(3) = 134.0 (2), m(3)-Ir(1)-N(1) = 114.8 (2), and N(1)-Ir(1)-m(1) = 110.0 (3)°. The Sn(1)-Br(1) bond is twisted 24° around Ir(1)-m(3) out of the equatorial

Figure 2. X-ray structure of Ir[C₆H₃(CH₂NMe₂)₂-2,4](COD) (7).⁸

plane. The nontrivial implications of this geometry and the resulting bonding description are dealt with in the Discussion.

The distance from iridium to the midpoint of the axial double bond of COD [m(2)] is longer than that of the equatorial one [m(1)] [2.174 (8) versus 2.033 (8) Å], in accord with earlier observations on five-coordinated iridium(I) diene species.¹³ The former bond length is one of the longest iridium(I)-olefin bonds encountered so far. The geometry of the C,N-bonded aryl ligand in **2** resembles that in square-planar Ir[C₆H₃(CH₂NMe₂)₂-2,4](COD) (**7**), see X-ray structure in Figure 2.⁸ The Ir-C(aryl) distance of 2.072 (7) Å is close to that in **7** [2.070 (8) Å], but the Ir-N distance of 2.357 (7) Å is significantly longer than in **7** [2.164 (3) Å]. The geometrical constraints of this chelating

(12) Holmes, R. R. *Prog. Inorg. Chem.* **1984**, 32, 119.

(13) (a) Churchill, M. R.; Bezman, S. A. *Inorg. Chem.* **1972**, 11, 2243. (b) Churchill, M. R.; Bezman, S. A. *Inorg. Chem.* **1973**, 12, 260. (c) Churchill, M. R.; Bezman, S. A. *Inorg. Chem.* **1973**, 12, 531. (d) Porta, P.; Powell, H. M.; Mawby, R. J.; Venanzi, L. M. *J. Chem. Soc. A* **1967**, 455. (e) Churchill, M. R.; Lin, K. G. *J. Am. Chem. Soc.* **1974**, 96, 76. (f) Brunie, S.; Mazan, J.; Langlois, N.; Kagan, H. B. *J. Organomet. Chem.* **1976**, 114, 225.

Table V. Selected Bond Angles (deg) of [2-(Me₂NCH₂)C₆H₄](COD)Ir(Br)SnMe₂Br^a

	molecule 1	molecule 2
(a) Around Iridium		
Sn(1)–Ir(1)–Br(1)	68.51 (3)	68.26 (3)
Sn(1)–Ir(1)–N(1)	142.0 (2)	141.8 (2)
Sn(1)–Ir(1)–C(1)	81.8 (2)	81.2 (2)
Sn(1)–Ir(1)–m(1)	101.0 (2)	99.7 (2)
Sn(1)–Ir(1)–m(2)	101.1 (2)	102.5 (2)
Br(1)–Ir(1)–N(1)	84.1 (2)	84.0 (2)
Br(1)–Ir(1)–C(1)	97.6 (2)	96.6 (2)
Br(1)–Ir(1)–m(1)	164.8 (3)	163.9 (2)
Br(1)–Ir(1)–m(2)	86.7 (2)	88.1 (2)
N(1)–Ir(1)–C(1)	76.1 (3)	76.4 (3)
N(1)–Ir(1)–m(1)	110.0 (3)	111.4 (3)
N(1)–Ir(1)–m(2)	103.1 (3)	102.1 (3)
C(1)–Ir(1)–m(1)	91.4 (3)	91.9 (3)
C(1)–Ir(1)–m(2)	175.4 (3)	174.9 (3)
m(1)–Ir(1)–m(2)	84.7 (3)	84.1 (3)
N(1)–Ir(1)–m(3)	114.8 (2)	114.6 (2)
C(1)–Ir(1)–m(3)	89.6 (2)	88.6 (2)
m(1)–Ir(1)–m(3)	134.0 (2)	132.7 (2)
m(2)–Ir(1)–m(3)	94.8 (2)	96.4 (2)
Ir(1)–Br(1)–Sn(1)	56.52 (3)	56.57 (3)
(b) Around Tin		
Ir(1)–Sn(1)–Br(1)	54.97 (3)	55.17 (3)
Ir(1)–Sn(1)–Br(2)	116.35 (4)	116.59 (4)
Ir(1)–Sn(1)–C(10)	117.4 (3)	116.7 (3)
Ir(1)–Sn(1)–C(11)	117.4 (2)	116.5 (2)
Br(1)–Sn(1)–Br(2)	169.47 (4)	170.87 (4)
Br(1)–Sn(1)–C(10)	85.9 (3)	88.1 (3)
Br(1)–Sn(1)–C(11)	93.3 (2)	92.3 (2)
Br(2)–Sn(1)–C(10)	94.3 (3)	93.2 (3)
Br(2)–Sn(1)–C(11)	96.5 (2)	95.4 (2)
C(10)–Sn(1)–C(11)	110.7 (3)	114.2 (3)
(c) Within Aryl Ligand		
⟨C–N(1)–C⟩	107.0 (9)	107.2 (4)
Ir(1)–N(1)–C(7)	101.5 (5)	102.3 (5)
Ir(1)–N(1)–C(8)	114.8 (5)	113.4 (5)
Ir(1)–N(1)–C(9)	118.0 (5)	118.7 (5)
Ir(1)–C(1)–C(2)	115.7 (5)	114.4 (6)
Ir(1)–C(1)–C(6)	128.1 (5)	129.3 (6)
C(2)–C(1)–C(6)	115.9 (6)	116.2 (7)
N(1)–C(7)–C(2)	109.7 (7)	108.8 (7)
(d) Within COD Ligand		
⟨C(sp ²)–C(sp ²)–C(sp ²)⟩	122.5 (4)	122.5 (9)
⟨C(sp ²)–C(sp ²)–C(sp ²)⟩	114.4 (9)	114.5 (5)

^am(1) is the midpoint of C(14)–C(15), m(2) is the midpoint of C(18)–C(19), and m(3) is the midpoint of Sn(1)–Br(1).

organic ligand impose an acute N(1)–Ir(1)–C(1) angle of 76.1 (3)° [compare 80.4 (2) in 7].

For **2** the distortion (D) from a trigonal bipyramid toward a square pyramid along the Berry pseudorotation coordinate is only 23%,¹² and in this respect it is surprisingly closer to a perfect trigonal bipyramidal geometry than other five-coordinate iridium(I) diene structures, such as IrMe(COD)(PMe₂Ph)₂ (D = 40%),^{13a} IrMe(COD)[Ph₂P(CH₂)₂PPh₂]₂ (D = 62%),^{13b} IrMe(COD)[Ph₂P(CH₂)₃PPh₂]₂ (D = 53%),^{13c} IrSnCl₃(COD)₂ (D = 48%),^{13d} IrSnCl₃(NBD)(PMe₂Ph)₂ (D = 78%),^{13e} and IrCl(COD)((+)-diop) (D = 41%).^{13f} As for **2** they all have an axially/equatorially coordinated diene ligand with, as anticipated, the most electronegative ligand in the other axial position.

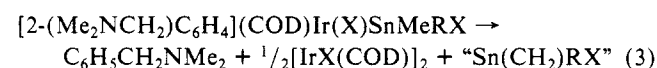
The formation of **2** from square-planar Ir[C₆H₄(CH₂NMe₂)₂](COD), whose structure will be similar to that of Ir[C₆H₃(CH₂NMe₂)₂,2,4](COD) (**7**, Figure 2),⁸ can be easily visualized. As the tin(IV) compound approaches for coordination to iridium, the straight C(aryl)–Ir–m(olefin) axis apparently remains intact, while the other double bond and the N-atom rotate toward each other about this axis, by ca. 65°, to form **2**.

Tin Coordination Sphere. As with the iridium atom the best practicable, though not perfect, description of the tin moiety is

based on a trigonal bipyramidal geometry. Around the tin atom, the two bromine atoms occupy the axial positions [Br(1)–Sn(1)–Br(2) = 169.47 (4)°], and the two carbon atoms of the methyl groups reside in the equatorial plane [C(10)–Ir(1)–C(11) = 110.7 (3)°]. The third position in this plane seems to be vacant; the Ir(1) atom lies closest to it, but the Sn(1)–Ir(1) vector lies 35° out of the equatorial plane toward Br(1). The two Sn–Br bond lengths show a marked difference; the Sn(1)–Br(1) bond, associated with bonding to Ir(1), is much longer than Sn(1)–Br(2) [2.934 (1) versus 2.608 (1) Å]. The latter distance is closer to, but somewhat shorter than, the normal range of 2.63–2.68 Å found for axial Sn–Br bonds in pentacoordinated tin compounds with trigonal bipyramidal geometries.¹⁴

Geometry of the Iridium–Tin Interaction. The salient feature of the structure of **2** is the rather regular triangle formed by Ir(1), Sn(1), and Br(1) [Sn(1)–Ir(1)–Br(1) = 68.51 (3), Ir(1)–Br(1)–Sn(1) = 56.52 (3), and Ir(1)–Sn(1)–Br(1); 54.97 (3)°]. The Ir–Sn distance of 2.6297 (8) Å lies within the normal range for single Ir–Sn bonds (2.59–2.64 Å).^{13d,e,15} The Ir–Br distance of 2.582 (1) also lies within the normal range of 2.52–2.64 Å found for this bond.¹⁶ The triangular geometry of the Ir–Sn–Br unit closely resembles that of M–Sn–X units in three other group 6 metal d⁶ complexes, i.e., (2,2′-bipyridine)(CO)₂Mo(Cl)SnMeCl₂ (**8a**),^{17a} [MeS(CH₂)₂SMel(CO)₃W(Cl)SnMeCl₂ (**8b**)],^{17b} and [MeS(CH₂)₂SMel(CO)₃Mo(Cl)SnCl₃ (**8c**)],^{17c} whose common structural features are depicted in Table VI. The striking geometrical similarities suggest that a common mode of bonding exists between the transition metal and tin fragments in all four species (see Discussion).

Stability of [2-(Me₂NCH₂)C₆H₄](COD)Ir(X)SnRR′X (1–6) and Reactions of Ir[C₆H₃(CH₂NMe₂)₂,2-R-6](COD) (R = Me, CH₂NMe₂) with SnMe₂Br₂. All adducts 1–6 are indefinitely stable in the solid state, while adducts **3** and **6** (which bear *no* Sn–Me bonds) are also stable in solution, even in the presence of a large excess of a coordinating solvent like pyridine. However, the other adducts **1**, **2**, **4**, and **5** (which do bear Sn–Me bonds) decompose within 1 day in either dichloromethane or benzene solutions. The decomposition of these complexes, which is a first-order process (*t*_{1/2} ≈ 10 h), results in the simultaneous formation of C₆H₅CH₂NMe₂ and [IrX(COD)]₂, together with some off-white precipitate (eq 3). On the basis of the products left in solution,



the insoluble precipitate must contain all of the tin and has the stoichiometry [Sn(CH₂)RX]_n. This material is possibly a polymer analogous to carboranes. For the formation of C₆H₅CH₂NMe₂ a hydrogen atom appears to be abstracted from an Sn–Me group of the starting iridium–tin adduct, since only those adducts bearing Sn–Me groups are prone to this decomposition. The mechanism of this reaction is unknown but could involve a kind of β-elimination.

(14) (a) Weichmann, H.; Mugge, C.; Grand, A.; Robert, J. B. *J. Organomet. Chem.* **1982**, 238, 343. (b) Allen, D. W.; Derbyshire, D. J.; Saratov, I. E.; Reikhsfel'd, V. O. *Kristallografiya* **1985**, 30, 297. (c) van Koten, G.; Noltes, J. G.; Spek, A. L. *J. Organomet. Chem.* **1976**, 118, 183. (d) Jastrzebski, J. T. B. H.; van Koten, G.; Knaap, C. T.; Schreurs, A. M. M.; Kroon, J.; Spek, A. L. *Organometallics* **1986**, 5, 1551.

(15) (a) Gilbert, T. M.; Hollander, F. J.; Bergman, R. G. *J. Am. Chem. Soc.* **1985**, 107, 3508. (b) Kretschmer, M.; Pregosin, P. S.; Albinati, A.; Togni, A. *J. Organomet. Chem.* **1985**, 281, 365.

(16) (a) Thorn, D. L.; Tulip, T. H. *J. Am. Chem. Soc.* **1981**, 103, 5984. (b) Behrens, U.; Dahlenburg, L. *J. Organomet. Chem.* **1976**, 116, 103. (c) Brotherton, P. D.; Raston, C. L.; White, A. H.; Wild, S. B. *J. Chem. Soc., Dalton Trans.* **1976**, 1799. (d) Von Deuten, K.; Dahlenburg, L. *Cryst. Struct. Commun.* **1980**, 9, 421. (e) Calabrese, J. C.; Roe, D. C.; Thorn, D. L.; Tulip, T. H. *Organometallics* **1984**, 3, 1223. (f) Johnson, C. E.; Eisenberg, R. J. *Am. Chem. Soc.* **1985**, 107, 3148. (g) Churchill, M. R.; Hackbarth, J. J. *Inorg. Chem.* **1975**, 14, 2047. (h) Teo, B. K.; Snyder-Robinson, P. A. *J. Chem. Soc., Chem. Commun.* **1979**, 255. (i) Churchill, M. R.; Julis, S. A. *Inorg. Chem.* **1979**, 18, 1215. (j) Ciani, G.; Manassero, M.; Sironi, A. *J. Organomet. Chem.* **1980**, 199, 271.

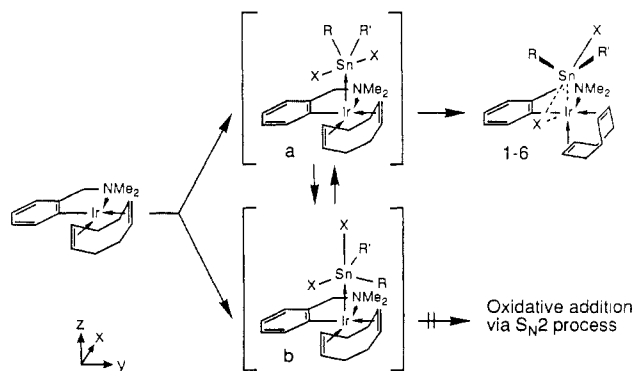
(17) (a) Elder, M.; Hall, D. *Inorg. Chem.* **1969**, 8, 1268. (b) Elder, M.; Hall, D. *Inorg. Chem.* **1969**, 8, 1273. (c) Anderson, R. A.; Einstein, F. W. B. *Acta Crystallogr., Sect. B: Struct. Crystallogr. Cryst. Chem.* **1976**, B32, 966.

Table VI. Selected Geometrical Data of **2** and **8a-c**^{17a}

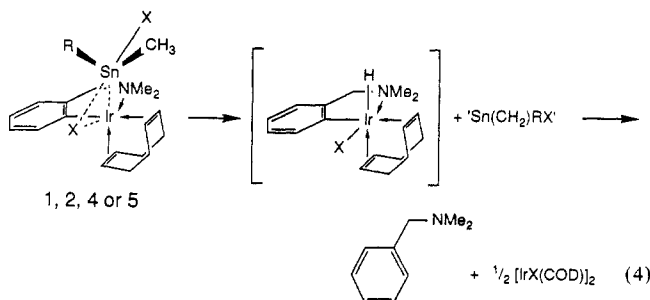
compound	Sn-M-X _{ax} triangle			X _{ax} -(Sn)-X _{ax'} axis			
	Sn-M-X _{ax}	M-X _{ax} -Sn	X _{ax} -Sn-M	X _{ax} -Sn-X _{ax'}	Sn-X _{ax}	Sn-X _{ax'}	
(2)	[2-(Me ₂ NCH ₂)C ₆ H ₄](COD)Ir(Br)SnMe ₂ Br	68.26 (4)	56.59 (4)	55.15 (3)	170.88 (5)	2.933 (2)	2.626 (2)
(8a)	(2,2'-bipyridine)(CO) ₃ Mo(Cl)SnMeCl ₂	63.6 (1)	61.6 (1)	54.8 (1)	168.1 (1)	2.805 (4)	2.433 (5)
(8b)	(MeSCH ₂ CH ₂ SMe)(CO) ₃ W(Cl)SnMeCl ₂	68.0 (2)	59.9 (2)	52.1 (2)	165.9 (3)	2.96 (1)	2.38 (1)
(8c)	(MeSCH ₂ CH ₂ SMe)(CO) ₃ Mo(Cl)SnCl ₃	64.3 (1)	60.5 (1)	55.2 (1)	172.9 (2)	2.781 (4)	2.381 (5)

^a Bond angles in deg; bond lengths in Å. X_{ax} is the tin-bonded axial halide that is also involved in bonding to either Ir, Mo, or W.

Scheme I



nation process of an Ir-Sn-CH₃ moiety, affording "Sn(CH₂)RX" and the intermediate IrHX[C₆H₄(CH₂NMe₂)-2](COD) (eq 4).



The bis-ortho-substituted aryl complexes Ir[C₆H₃(CH₂NMe₂)₂-2-R-6](COD) (R = Me, CH₂NMe₂) were also reacted with SnMe₂Br₂ in benzene. In these cases, no formation of Ir-Sn adducts was observed, but instead an instant decomposition to 1-(Me₂NCH₂)-3-R-C₆H₄ and [IrBr(COD)]₂ occurred (100% for R = Me, 65% for R = CH₂NMe₂). Apparently the same decomposition pathway is followed as for the mono-ortho-substituted complexes. However, the reaction time (a few seconds) is much shorter and must be due to the steric crowding that the R-group exerts in the presumed intermediate [6-R-2-(Me₂NCH₂)C₆H₃](COD)Ir(Br)SnMe₂Br.

For R = CH₂NMe₂ a competing transmetalation reaction occurred, resulting in 35% formation of {SnMe₂[C₆H₃(CH₂NMe₂)₂-2,6]}Br. In this respect, it is noted that the related complex Rh[C₆H₃(CH₂NMe₂)₂-2,6](COD) is known to react with SnMe₂Br₂ to afford 100% {SnMe₂[C₆H₃(CH₂NMe₂)₂-2,6]}Br (eq 5).⁷ This transmetalation reaction is thought to proceed via Rh[C₆H₃(CH₂NMe₂)₂-2,6](COD) + SnMe₂Br₂ → {SnMe₂[C₆H₃(CH₂NMe₂)₂-2,6]}Br + 1/2[RhBr(COD)]₂ (5)

electrophilic attack of the tin moiety on the Rh-C bond or on the C(aryl) atom but *not* on the rhodium center. In contrast, the similar reaction with the iridium complex appears to proceed mainly via the iridium center, i.e., by the intermediate formation of an Ir-Sn adduct and concomitant decomposition. This difference in behavior must, therefore, be attributed to the higher nucleophilicity of iridium with respect to rhodium.

Discussion

Formation of [2-(Me₂NCH₂)C₆H₄](COD)Ir(X)SnRR'X (1-6). The starting complexes Ir[C₆H₄(CH₂NMe₂)-2](COD) and SnRR'X₂ have a square-planar and a tetrahedral geometry around the metal, respectively, but both end up as trigonal bipyramids

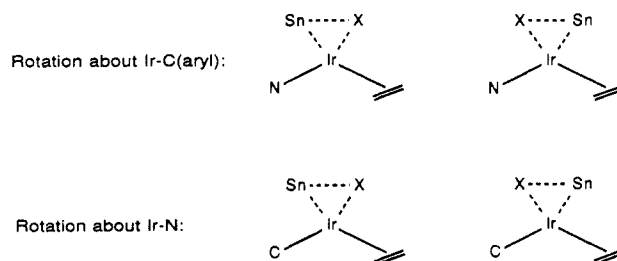


Figure 3. Possible stereoisomers of [2-(Me₂NCH₂)C₆H₄](COD)Ir(X)SnRR'X (1-6).

in the final products **1-6**. In discussing the consequences of these geometrical changes from an MO point of view, the *x* and *y* axes are taken as approximately colinear with the respective Ir-N and Ir-C(aryl) bonds of the starting iridium(I) complex, and the *z* axis is perpendicular to the coordination plane (Scheme I).

The First Step. The primary interaction of SnRR'X₂ with the iridium center of Ir[C₆H₄(CH₂NMe₂)-2](COD) occurs along the *z* axis and can take place through either a halide atom, a tin-halide bond, or the tin atom. The first two possibilities are seen to be unlikely because the HOMO of the starting iridium(I) complex, being a mainly metal localized d_{z²} orbital, will encounter a strong anti-bonding interaction with filled orbitals of the same symmetry on the tin species. Therefore, the primary interaction is likely to be of a Lewis acid-base type through the filled d_{z²} orbital of iridium and an empty orbital of tin, see Scheme I. This is corroborated by the experimental observation that on increasing the number of halide atoms on tin, and hence the Lewis acidity of the tin(IV) center, the adduct formation proceeds more readily. This type of interaction would also explain why the weaker Lewis acid SnMe₃Cl does not form an adduct under the conditions employed.

In order to bond with the iridium complex, the tin species has to rehybridize from a tetrahedral (sp³) to a trigonal bipyramidal (sp³d) arrangement by admixture of an empty 5d orbital. The bonding of the five-coordinate tin center will then be directed in such a way as to accommodate the more electronegative atoms (halide atoms) in axial and the better σ-donor (iridium atom) in equatorial positions.¹⁸ At the same time the coordination around iridium will change toward square pyramidal. Two intermediate structures, differing by their arrangement of tin-bonded substituents, can be put forward (**a** and **b** in Scheme I). This difference is of minor importance, since for following steps these structures can probably interchange readily via low barrier, Berry rotations around the tin atom.¹⁹ Although structure **b** appears well suited to react further by means of an S_N2 type oxidative addition process, involving breakage of the axial tin-halide bond, it does not do so. This process, however, probably does operate in the trans oxidative addition of a tin-halide bond of SnR₃X to the metal d⁸ complex Pt^{II}Me₂(N-N) (N-N = 2,2'-bipyridine and 1,10-phenanthroline).²⁰ Stable dinuclear metal d⁸→d¹⁰ Lewis acid-base adducts of the type described above have not as yet been reported with tin(IV) compounds, but they are known with mercury(II) salts, e.g., [2,6-(Me₂NCH₂)₂C₆H₃]Pt[μ-(*p*-tol)NC(H)N(*i*-Pr)]HgBrCl.²¹

(18) Bent, H. A. *Chem. Rev.* **1961**, *61*, 275.

(19) Shapley, J. R.; Osborn, J. A. *Acc. Chem. Res.* **1973**, *6*, 305.

(20) Kuyper, J. *Inorg. Chem.* **1977**, *16*, 2171.

(21) van der Ploeg, A. F. M. J.; van Koten, G.; Vrieze, K.; Spek, A. L.; Duisenberg, A. J. M. *Organometallics* **1982**, *1*, 1066.

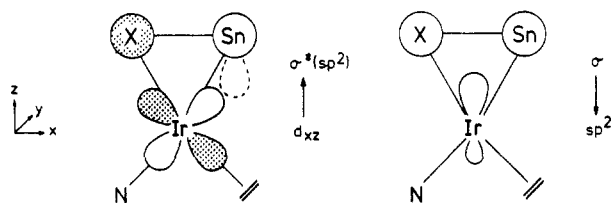


Figure 4. Bonding interaction between the iridium and tin moieties in $[2-(\text{Me}_2\text{NCH}_2)_2\text{C}_6\text{H}_4](\text{COD})\text{Ir}(\text{X})\text{SnRR}'\text{X}$ (**1-6**).

The Second Step. The bonding between the iridium and tin moieties in the final products **1-6** is clearly different from that in the preceding Lewis acid–base adduct, described above. It seems likely that starting from this initial interaction a concerted process takes place in which the iridium moiety migrates from tin toward the tin–halide bond. As such this migration can be regarded as the first stage of a concerted cis oxidative addition of a tin–halide bond to an iridium(I) center, and the present complexes (**1-6**) can therefore be considered as “trapped” intermediates in this process.

This migration can, in principle, give rise to four stereoisomers, although only one is observed (Figure 3). Firstly, to enable coordination of a tin–halide bond to iridium, rotation of the aryl ligand (in the xz plane, z intersecting the vector of the rotating ligands) about the Ir–C(aryl) axis occurs and *not* about the Ir–N axis. This exclusive rotation about Ir–C(aryl), also realized during the reaction of $\text{Ir}[\text{C}_6\text{H}_4(\text{CH}_2\text{NMe}_2)_2](\text{COD})$ with dihydrogen,⁶ seems to be directed by repulsive forces within the complex. Secondly, although the iridium-coordinated tin–halide bond can in principle orient itself in two ways in the equatorial (xz) plane, the tin atom is directed opposite to the in-plane N atom, which has a larger trans influence than the COD double bond.

Upon migration of the iridium moiety toward a tin–halide bond the amine group and the other COD double bond bend ca. 65° toward each other, resulting in the formation of a bent $d^8 \text{ML}_4$ arrangement. This bending destabilizes the d_{xz} orbital of iridium, which now becomes the HOMO of the iridium moiety, and stabilizes the d_{z^2} orbital. While the donative interaction of the d_{z^2} orbital with a tin sp^2 hybrid decreases, the π -interaction of the d_{xz} orbital with the σ^* orbital of the tin–halide bond increases (it is possible that this tin sp^2 hybrid, pointing more or less toward iridium, remains involved in the bonding in the final adduct) (Figure 4). In this respect, it should be recalled that the coordinated Sn–X bond in the adducts **1-6** (cf. Sn–Br in the X-ray structure of **2**) lies approximately in the equatorial (xz) plane, an orientation that is calculated to be optimal for π -overlap.²¹ Additionally, the LUMO of the bent iridium moiety, being an orbital of approximate sp^2 symmetry, can, in a kind of “backbonding”, accept electrons from the σ orbital of the tin–halide bond (Figure 4). The final bonding description is very similar to that of the classical example of the interaction of an olefin with the bent $\text{Fe}(\text{CO})_4$ fragment,²² whose frontier orbitals are isolobal with the bent $\text{Ir}[\text{C}_6\text{H}_4(\text{CH}_2\text{NMe}_2)_2](\text{COD})$ moiety.

Except for the side-on coordinated hydrogen molecule, the σ and σ^* orbitals of diatomic substrates in general lie respectively too low and too high in energy for a significant overlap with metal orbitals.²³ However, in the present case it can be anticipated that the rehybridization of tin orbitals upon changing from a tetrahedral to a trigonal bipyramidal geometry will produce weakened axial bonds and so bring the σ and σ^* orbitals closer in energy to the frontier orbitals of iridium.

The Third Step. Starting from the adducts **1-6**, oxidative addition of the tin–halide bond (i.e., formation of two Ir–X and Ir–Sn single bonds) is expected to be the next reaction step. The fact that this does not happen, in contrast to a number of other cases,^{3,18,24} may be ascribed in part to steric crowding. This

explanation was also put forward for the formation of the complexes $(\text{LL})(\text{CO})_3\text{M}(\text{X})\text{SnRR}'\text{X}$ (**8a-c**, LL = bidentate S or N ligand, M = Mo, W) that contain a nearly identical M–Sn–X triangle, from $\text{M}(\text{LL})(\text{CO})_4$ and $\text{SnRR}'\text{X}_2$.¹⁷ However, factors other than those of steric origin must also play a role since in other similar cases, such as the reaction of $\text{W}(2,2'\text{-bipyridine})(\text{CO})_4$ with GeBr_4 , a true seven-coordinate oxidative addition product *does* form.²⁵ As observed earlier, there are striking structural similarities, regarding the M–Sn–X triangles (Table VI), between our iridium–tin adducts (**1-6**) and the molybdenum/tungsten–tin adducts (**8**). Since the transition-metal fragments involved in these adducts (bent $d^8\text{-ML}_4$ in **1-6** and $d^6\text{-ML}_5$ in **8**) are isolobal, it is to be expected that common electronic factors govern the choice between side-on coordination or oxidative addition of the tin–halide bond.

This choice has recently been discussed in a quantitative way for dihydrogen, for which both examples of η^2 coordination and oxidative addition are known.²⁶ Ab initio studies on the WL_3H_2 system showed that reduced π overlap between the metal d_{xz} and the dihydrogen σ^* orbital prevents oxidative addition and hence stabilizes side-on coordination of dihydrogen instead. In the present iridium–(and molybdenum/tungsten–)tin complexes it can be argued that a similar overlap “imbalance” exists between the frontier orbitals of the transition metal and the σ and σ^* orbitals of the Sn–X bond, for which there is little σ and π synergistic interaction that would drive the system to concerted cis oxidative addition.

Another factor of relevance in the discussion of the M–Sn–X triangle is the significant degree of π -character in a tin–halide bond arising from donation of filled p orbitals of the halide atoms to empty 5d orbitals on tin.²⁷ Although this interaction is relatively weak, compared to that of the σ -bond, it is possible that in **1-6** and **8** it is just this extra tin–halide bonding, which stabilizes (in cooperation with steric factors) the three-center M–Sn–X interaction with respect to an oxidative addition product.

More Analogies. The iridium moiety in **1-6**, being a bent $d^8 \text{ML}_4$ fragment, is not only isolobal with the $d^6 \text{ML}_5$ fragment (as in **8**) but also with T-shaped $d^8 \text{ML}_3$, bent $d^{10} \text{ML}_2$, and the methylene group.

The mechanism of the cis oxidative addition of tin–halide bonds to several platinum(0) complexes of the bent $d^{10} \text{ML}_2$ type²⁴ may well involve an intermediate having a Pt–Sn–X triangle analogous to that in **1-6** and **8**.

From the isolobal point of view, the tin(IV) compounds $\text{Sn}(\text{CH}_2\text{X})\text{R}_3$, which bear a methyl group α -substituted by a halide atom are also interesting. These compounds are thought to possess intramolecular coordination of the halide X to tin,²⁸ but this situation can also be regarded as an example of a tin–halide bond that is side-on coordinated to a methylene group.

As well as tin, other group 14 elements can be involved in side-on bonding. For example, complexes of the type $\text{Cp}(\text{CO})_2\text{Mn}(\text{H})\text{SiRR}'\text{R}''$, in which the Si–H bond acts as side-on coordinated ligand, can be regarded as “trapped” intermediates in hydrosilylation reactions.²⁹ However, in contrast to the tin atom in **1-6** (and **8**), the silicon atom in these manganese complexes are found to be tetrahedral. Finally, the analogy that exists between side-on coordinated Sn–X and Si–H bonds and agostic C–H bonds should be mentioned,³⁰ especially in the light of the

(25) Cradwick, E. M.; Hall, D. *J. Organomet. Chem.* **1970**, *25*, 91.

(26) Hay, P. J. *J. Am. Chem. Soc.* **1987**, *109*, 705.

(27) Bertocello, R.; Daudey, J. P.; Granozzi, G.; Russo, U. *Organometallics* **1986**, *5*, 1866.

(28) (a) Egorochkin, A. N.; Sevastyanova, E. I.; Khorshev, S. Y.; Ratushnaya, S. K.; Richelme, S.; Satge, J.; Riviere, P. *J. Organomet. Chem.* **1980**, *188*, 73. (b) Egorochkin, A. N.; Sevastyanova, E. I.; Khorshev, S. Y.; Richelme, S.; Satge, J. *J. Organomet. Chem.* **1981**, *205*, 311, references cited therein.

(29) (a) Hutcheon, W. L. *Chem. Eng. News* **1970**, *48*, 75. (b) Carre, F.; Colomer, E.; Corriu, R. J. P.; Vioux, A. *Organometallics* **1984**, *3*, 1272. (c) Schubert, U.; Ackermann, K.; Kraft, G.; Woerle, B. *Z. Naturforsch., B: Anorg. Chem., Org. Chem.* **1983**, *38B*, 1488. (d) Schubert, U.; Kraft, G.; Walther, E. *Z. Anorg. Allg. Chem.* **1984**, *519*, 96. (e) Schubert, U.; Scholz, G.; Mueller, J.; Ackermann, K.; Woerle, B. *J. Organomet. Chem.* **1986**, *306*, 303.

(22) Hoffmann, R. *Science (Washington, D.C.)* **1981**, *211*, 995.

(23) Saillard, J.; Hoffmann, R. *J. Am. Chem. Soc.* **1984**, *106*, 2006.

(24) (a) Eaborn, C.; Pidcock, A.; Steele, B. R. *J. Chem. Soc., Dalton Trans.* **1976**, 767. (b) Butler, G.; Eaborn, C.; Pidcock, A. *J. Organomet. Chem.* **1979**, *181*, 47.

recent detection of η^2 -coordinated C-H bonds by Bergman et al.³¹

Conclusions

The special arrangement of ligands in square-planar Ir-[C₆H₄(CH₂NMe₂)₂](COD) has resulted in the isolation of unique adducts with organotin(IV) halides that can be regarded as "trapped" three-center intermediates in the oxidative addition of a metal-halide bond to metal d⁸ complex. It can be anticipated, based on isolobal relationships, that many new transition-metal complexes having side-on coordinated (main group) M-X bonds can be synthesized not only with tin(IV) (or other group 14 elements) but also with d¹⁰ metals like thallium(III), mercury(II), and gold(I).

Acknowledgment. X-ray data were kindly collected by A. J. M. Duisenberg. This work was supported in part (W.J.J.S. and

A.L.S.) by the Dutch Foundation for Chemical Research (SON) with financial aid from the Dutch Organization for Advancement of Pure Research (ZWO).

Registry No. 1, 115076-05-6; 2, 115076-06-7; 3, 115076-07-8; 4a, 115076-08-9; 4b, 115116-29-5; 5, 115076-09-0; 6, 115076-10-3; Ir-[C₆H₄(CH₂NMe₂)₂](COD), 114762-91-3; SnMe₂Cl₂, 753-73-1; SnMe₂Br₂, 2767-47-7; SnPh₂Cl₂, 1135-99-5; SnMePhBr₂, 21247-36-9; SnMeCl₃, 993-16-8; SnBr₄, 7789-67-5; [IrBr(COD)]₂, 12245-73-7; [C₆H₃CH₂NCHMe₂Cl], 1875-92-9; Ir[C₆H₃(CH₂NMe₂)₂-2-Me-6](COD), 114762-90-2; Ir[C₆H₃(CH₂NMe₂)₂-2-CH₂NMe₂-6](COD), 114762-89-9; [1-(Me₂(H)NCH₂)-3-Me-C₆H₄]Cl, 115031-97-5; [1,3-(Me₂(H)NCH₂)₂C₆H₄]Cl₂, 63400-16-8; [SnMe₂[C₆H₃(CH₂NMe₂)₂-2,6]Cl], 115092-11-0.

Supplementary Material Available: Tables of anisotropic thermal parameters and all H-atom parameters and a complete list of bond lengths and bond angles (7 pages); listing of observed and calculated structure factor amplitudes (46 pages). Ordering information is given on any current masthead page.

(30) Brookhart, M.; Green, M. L. H. *J. Organomet. Chem.* **1983**, 250, 395.

(31) Periana, R. A.; Bergman, R. G. *J. Am. Chem. Soc.* **1986**, 108, 7332.

Defect Patterns in Perovskites

Jeremy K. Burdett* and Gururaj V. Kulkarni

Contribution from the Chemistry Department, The University of Chicago, Chicago, Illinois 60637. Received December 9, 1987

Abstract: The method of moments is used to understand the results of molecular orbital calculations and tight-binding calculations on solids, designed to probe the reasons behind the ordering problem of defects in solids. This is a problem that can be regarded as the solid-state equivalent of the isomerization question in molecular chemistry. The structural preferences for *cis*- and *trans*-dioxo transition-metal complexes and the "defect patterns" predicted for binuclear vertex-sharing octahedral complexes of stoichiometry M₂L₉ are used to build a simple model that may be easily applied to the case of transition-metal-containing perovskites. The calculations and the model give a ready explanation for the observed ordering pattern in CaMnO_{2.5} and defect structures with fewer oxygen vacancies.

One of the important aspects of the geometrical structure of molecules is, of course, the stability of isomers of various types. Rotational isomerism in organic chemistry and the relative stability of *cis* and *trans* isomers in transition-metal chemistry come immediately to mind. Often the stability of the two structures varies with electron count. For example, *cis*-dioxo complexes are exclusively found for d⁰ metal centers but the *trans* isomer for d² systems. Often the predicted properties of the two isomers are very different, and this point underscores the often striking dependence of properties on structure. Seemingly minor geometrical variations often lead to very different properties.

Ordering patterns in molecules are important too. Given a collection of atoms that are to be assembled into a molecule of a set shape, what influences the choice of atomic connectivity? For example, in the structure of nitrous oxide, the oxygen atom is found in a terminal rather than central position. The most stable "coloring" pattern changes too with electron count. In the A₂O oxides, for molecules with 8-12 electrons (Li₂O, Ga₂O, for example) the oxygen atom is centrally located in contrast to the 16-electron case of N₂O.

In this paper we will study a problem of very basic chemical importance in the condensed phase. We will present a theoretical way to understand the ordering patterns of defects in solids. Our model will be applied initially to systems derived from the perovskites, materials of composition ABO₃.¹ Such defect structures give us a solid-state equivalent of the isomerism problem of the molecular chemist. Here we wish to understand what influences

their relative stabilities. Throughout our analysis we shall make extensive analogies with molecular problems. The major thrust in this paper will be to understand the atomic arrangement in the material CaMnO_{2.5} and other related systems with slightly higher oxygen content. Elsewhere we extend the picture to structures with lower oxygen content (O_{2.33}), which have recently been found to be high T_c superconductors.²⁻⁴ We will use one-electron orbital models which have proven immensely useful in almost all areas of chemistry, and will find the method of moments especially useful in understanding the variation in structural stability with electron count.

Defects in CaMnO₃

The chemist's view of defect structures is one that has changed over the years.⁵⁻⁷ Many of the structures, that carried this label years ago are now recognized as chemically distinct phases. If the number of defects is rather small (such as the Schottky defects

(2) Wu, M. K.; Ashburn, J. R.; Torng, C. J.; Hor, P. H.; Meng, R. L.; Gao, L.; Huang, Z. J.; Wang, Y. Q.; Chu, C. W. *Phys. Rev. Lett.* **1987**, 58, 908.

(3) Cava, R. J.; Batlogg, B.; van Dover, R. B.; Murphy, D. W.; Sunshine, S.; Siegrist, T.; Remeika, J. P.; Rietman, E. A.; Zahurak, S.; Espinosa, G. P. *Phys. Rev. Lett.* **1987**, 58, 1676.

(4) Schuller, I. K.; Hinks, D. G.; Beno, M. A.; Capone, D. W.; Soderholm, L.; Loquet, J.-P.; Bruynseraede, Y.; Segre, C. U.; Zhang, K. *Solid State Commun.* submitted for publication.

(5) A survey is given in Clark, G. M. *The Structures of Non-Molecular Solids*; Applied Science: London, 1972.

(6) West, A. R. In *Solid State Chemistry and Its Applications*; Wiley: New York, 1984; Chapters 9 and 10.

(7) Rao, C. N. R.; Gopalakrishnan, J. In *New Directions in Solid State Chemistry*; Cambridge University Press: Cambridge, 1986; Chapter 5.

(1) Smyth, D. M. *Annu. Rev. Mater. Sci.* **1985**, 15, 329.